

EVALUATION OF THE BACKGROUND COUNTING RATE IN A BALLOON-BORNE CODED APERTURE MASK TELESCOPE

A. Owens, D. Bhattacharya, E. L. Chupp, P. P. Dunphy,
M. L. McConnell and A. Bui-Van

University of New Hampshire, Durham, NH 03824, USA

1. Introduction. Because of the low source fluxes and high instrumental backgrounds typical of γ -ray astronomy, the minimum flux that can be measured by a telescope is at present ultimately limited by the level of the instrumental background. Therefore, a good understanding of the detector counting rate is essential if a realistic attempt is to be made to increase the instrumental sensitivity. In this paper we derive the various contributions to the counting rate of a coded aperture mask telescope. The instrument [1] is shown schematically in Figure 1 and consists of an array of 35 bismuth germanate (BGO) detectors actively shielded from below and on the sides by 10 cm of NaI(Tl). Each BGO detector is a right-circular cylinder of diameter 5.1 cm and thickness 2 cm. Located above, and parallel to, the detection plane is a 1.9 cm thick Pb coded aperture mask based on a 5×7 element Uniformly Redundant Array (URA). The fully coded field-of-view defined by the mask is $15.2^\circ \times 22.8^\circ$. The instrument covers the energy range 160 keV to 9.3 MeV and has a spectral resolution of 19% at 662 keV.

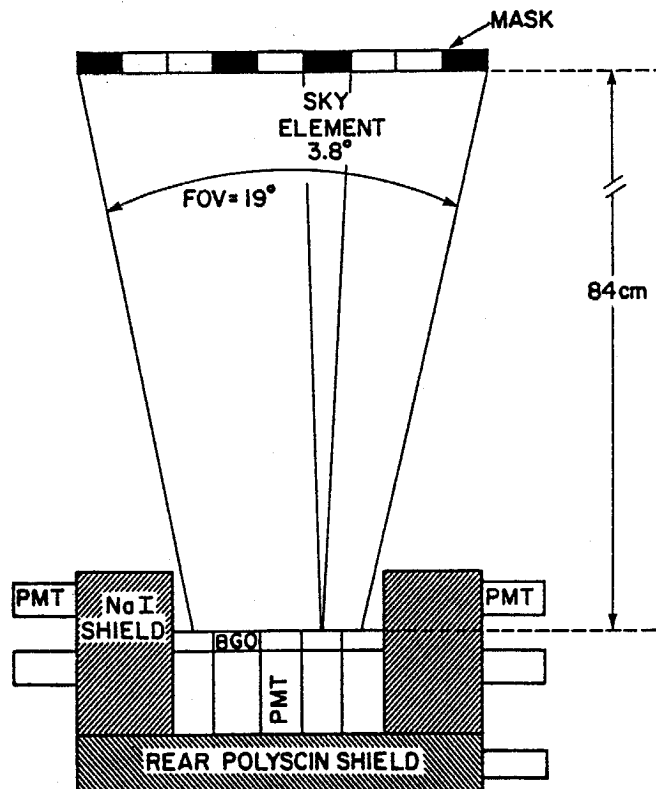


Figure 1.

2. Calculations and Results. The background counting rate in the telescope has been evaluated using Monte-Carlo and semi-empirical calculations and is compared to the experimentally measured energy-loss spectrum in Figure 2. These experimental data were obtained during a balloon flight on October 1, 1984 over Palestine, Texas at a mean float altitude of 3 g cm^{-2} . The model used in the present calculations is similar to that proposed by Dean and Nikiforidis [2]. The calculation proceeds in two parts. The upper 2π of the detection plane is considered unshielded and the various input radiation spectra are incident directly onto the detection plane. Note, that corrections are made for the presence of the coded aperture mask (which subtends $\sim 0.1 \text{ sr}$ at

the detection plane) and also for the thin pressure dome which covers the aperture. In order to calculate the counting rate due to radiation incident on the lower 2π sr, the telescope is approximated by a single rectangular BGO detector of dimensions, $35\text{ cm} \times 25\text{ cm} \times 2\text{ cm}$, surrounded by a series of concentric spherical shells representing the anticoincidence shield and additional materials surrounding the detection plane. The results are later normalized according to the actual detector volume and area. From Figure 2 it can be seen that the calculated and measured energy loss spectra are in reasonable agreement. The typical uncertainty in these calculations is estimated to be $\sim 30\%$. The various contributions to the detector energy-loss spectrum are described below.

Atmospheric and cosmic diffuse component: These components are due to the cosmic diffuse and atmospheric γ rays which enter the forward aperture, or pass through the shields, and deposit energy in the BGO array. The incident photons or their secondaries may interact in the shield undetected, provided that the total energy deposited is less than the shield threshold (250 keV). The flux and angular distribution of the atmospheric γ rays used in the calculation were taken from the parameterized forms given in Costa *et al.* [3]. The cosmic diffuse spectrum was taken from Schönfelder *et al.* [4].

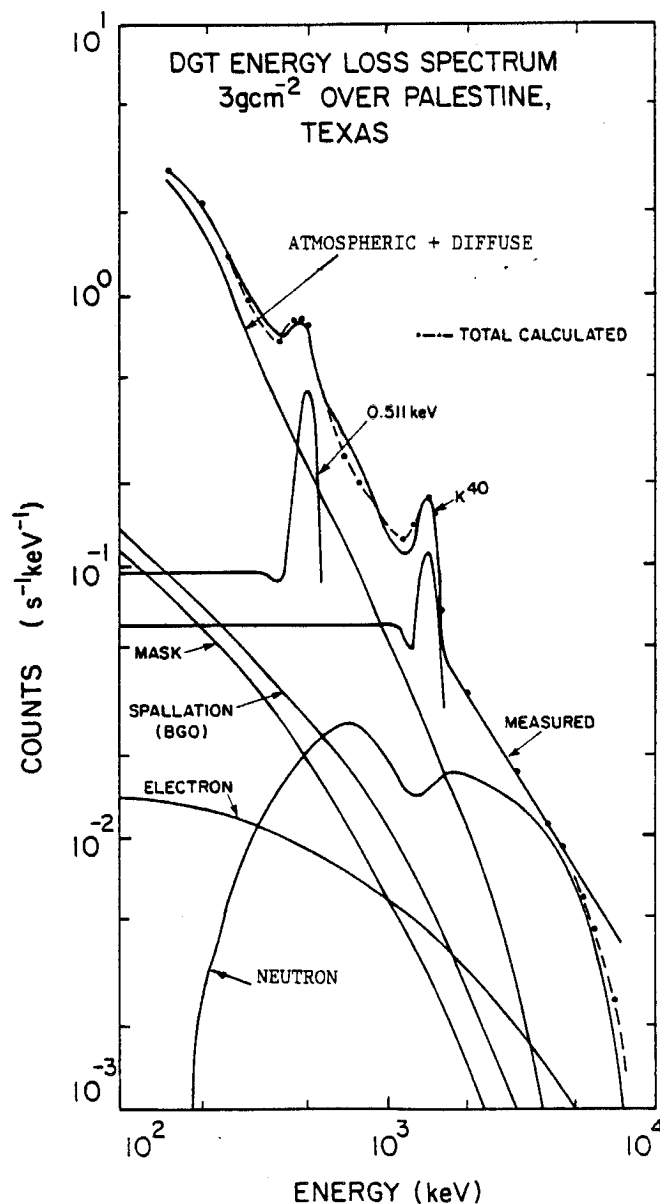


Figure 2.

Neutron induced component: Neutrons interact with the detector and shield material to produce γ rays through processes of capture or inelastic scattering. In the DGT, the neutron induced background dominates the detector counting rate at energies > 2 MeV.

The neutrons themselves may be classified into two distinct groups depending upon whether they were produced externally or internally to the instrument. The external neutrons are produced in the atmosphere by the interactions of the primary cosmic rays with air nuclei. The internal neutrons are produced primarily by evaporation from the nuclei of the instrument itself, following cosmic-ray initiated intranuclear cascades. In order to evaluate the production rate of background events due to external neutrons we have used the atmospheric neutron flux given in Dean and Dipper [5]. The internal neutron contribution was calculated by integration over the volume of the payload using the mean number of cascade and evaporation neutrons given in Bertini [6] and Powell *et al.* [7].

The principal contribution to the neutron induced counting rate arises from neutron interactions within the central array. In BGO, the contribution due to neutron capture reactions is approximately an order of magnitude smaller than that due to inelastic scattering and may, therefore, be neglected.

At low neutron energies (above ~ 100 keV) several discrete states are strongly excited by $(n, n' \gamma)$ giving rise to identifiable γ -ray lines in the spectrum. The strong broad group near 600 keV is attributed to several transitions in the Ge isotopes whereas the peaks at 0.9 and 1.6 MeV result mainly from first and second excited states of ^{209}Bi . As the neutron energy increases, the discrete transitions become less discernable, due to the increasing probability of multiple γ -ray emission. To calculate this component we have used radiative yields given in Hausser *et al.* [8].

Neutrons may also interact with the shield to produce radioactive nuclei which decay by emitting γ rays. The main contribution to the energy-loss spectrum arises from radiative capture on ^{127}I and from the decay of excited states of $^{127}\text{I}^*$ produced by inelastic scattering. In order to derive the contribution from this component, we have used the $\text{NaI}(\text{Tl})$ γ -ray yields computed by Ling and Gruber [9] and the experimental data of Shafroth *et al.* [10].

Spallation components: High-energy cosmic-rays may interact in the shield and central detector producing radioactive nuclides which decay in a time longer than the anticoincidence veto time of the instrument ($\sim 1 \mu\text{s}$). In $\text{NaI}(\text{Tl})$, the induced counting rate is well described by the empirical formula of Fishman [11] based on the Rudstam formula [12] for intermediate mass targets. The resulting γ -ray spectrum exhibits an exponential continuum in analogy with the spectrum produced from a large number of fission fragments [13]. The Fishman formula has also been evaluated for the central array assuming that the production of γ rays per gm in BGO is similar to that of iodine. This is a reasonable assumption since, to a first approximation, the average atomic weight distribution of fission products (and therefore nuclear energy level spacing) is close to that of Bi or Ge. A proton flux of $0.4 \text{ protons cm}^{-2} \text{ s}^{-1}$ at a rigidity of 4.5 GV was used in the calculations [14].

Mask component: Neutrons may also interact with the mask material to produce observable γ -ray fluxes at the detection plane. We have calculated this component using the γ -ray production yields given in Butler *et al.* [15]. As well as attenuating the incident γ -radiation, the mask will also act a secondary radiator. High-energy γ rays incident on the mask may Compton scatter or produce pairs within the mask material. The electron(s) can then produce secondary photons by bremsstrahlung, or (if an electromagnetic cascade is induced) by the secondary or tertiary electrons. The resulting γ -ray spectrum at the detection plane due to the secondary photons which escape from the mask was estimated from yields given in Owens *et al.* [16].

Electron and proton aperture flux: Primary and secondary electrons and protons may enter the forward instrument aperture and deposit energy in the detector. The incident electron flux was obtained from Daniel and Stephens [17]. In the case of the DGT, the electron background contribution is significant only at lower energies. The contribution due to soft albedo protons may be neglected since the incident flux is at least two orders of magnitude smaller than that of the electrons.

Natural Radioactivity: Some materials used in γ -ray detectors contain the natural radionuclides ^{40}K , Ra and Th which produce numerous emissions, both continuous and discrete, at γ -ray energies. The dominant emission of this type in the DGT is ^{40}K which decays by β^- emission to ^{40}Ca , or alternately to ^{40}Ar by β^+/EC decay, resulting in a γ -ray line at 1.46 MeV. After subtraction of the other contributions to the energy-loss spectrum, this component (along with that due to the atmospheric 511 keV line) was fit using the known photofraction of the BGO array.

3. Acknowledgments. We thank M. Chupp for editing and S. Cote and K. Dowd for typing the manuscript. This work was supported by NASA Grant NGL 30-002-021.

References

1. McConnell, M. L. *et al.*: 1983, *Adv. in Space Res.* **3**, 105.
2. Dean, A.J. and Nikiforidis: 1976, *Astr. and Ap.* **52**, 409.
3. Costa, E. *et al.*: 1984, *Ap. Space Sci.* **100**, 165.
4. Schönfelder, V. *et al.*: 1980, *Ap. J.*, **240**, 350.
5. Dean, A.J. and Dipper, N.A.: 1981, *Mon. Not. R. Astr. Soc.*, **194**, 219.
6. Bertini, H.W.: 1972, *Phys. Rev. C*, **6**, 631.
7. Powell, C.F. *et al.*: 1959, *The Study of Elementary Particles by the Photographic Method*, (New York:Pergamon Press).
8. Hausser, O. *et al.*: 1983, *Nucl. Instr. and Meth.*, **213**, 301.
9. Ling, J.C. and Gruber, D.E.: 1977, *J. Geophys. Res.*, **82**, 1211.
10. Shafroth, S.M. *et al.*: 1958, *Nucl. Instr. and Meth.*, **3**, 298.
11. Fishman, G.J.: 1972, *Ap. J.*, **171**, 163.
12. Rudstam, G.: 1966, *Zs. f. Naturforschung*, **21a**, 1027.
13. Goldstein, H.: 1959, *Fundamental Aspects of Reactor Shielding*, (Reading:Addison Wesley Co.) p. 60.
14. McDonald, F.B. and Webber, W.R.: 1958, *Phys. Rev.*, **115**, 194.
15. Butler, R.C.: 1984, *Nucl. Instr. and Meth.*, **221**, 41.
16. Owens, A. *et al.*: 1985, *Proc. of the 19th ICRC* **3**, 314.
17. Daniel, R.R. and Stephens, S.A.: 1974, *Rev. Geophys. and Space Phys.*, **12**, 233.